MODERNIZATION OF THE OUTFLOW SYSTEM OF CROSS-FLOW TURBINES

MACIEJ KANIECKI

Institute of Fluid-Flow Machinery,
Polish Academy of Sciences,
Fiszera 14, 80-952 Gdansk, Poland
kaniecki@imp.gda.pl

(Received 23 July 2001; revised manuscript received 5 April 2002)

Abstract: The presented article brings general overview of CFD analysis of two cross-flow turbine types (a classical impulse turbine and a reaction turbine). The author focuses his attention mainly on the discussion of differences in flow patterns in the outflow section of these turbines, because this element exerts significant impact on performance properties of the turbine. The article presents a comparison of computations and experimental results of the cross-flow turbine manufactured by IMP PAN. The analysis was performed by means of a computer program FLUENT 5.0™ for a two-dimensional example.

Keywords: cross-flow turbine, CFD analysis, outflow system

1. Introduction

The first cross-flow turbine was constructed by an Australian engineer A. Michell in 1903. However, a Hungarian professor D. Banki, who received a patent on a cross-flow turbine of his own design from the German Patent Department, created a theoretical basis for this type of machines. Application of these hydraulic turbomachines

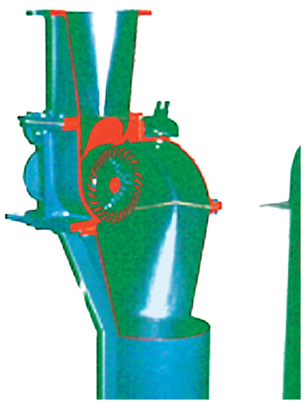

Figure 1. One of the oldest constructions of a cross-flow turbine, German Museum of Natural Sciences and Technology, Munich

became very popular already in 1917–1919, as it was mentioned in [1]. The new design filled the gap which existed between the application ranges of Francis and Pelton turbines. Nowadays, Banki-Michell turbines are often used in small hydro power plants, especially because of the economical aspect (low manufacture and operating costs).

During the whole last century the original design was systematically developed. However, the crucial changes in the original layout were introduced by a Czech engineer M. Cink who replaced ventilation of the runner casing, equipped his cross-flow turbine with a draft tube and replaced the guide vane with a cylindrical segment. All these design provisions eliminated the most negative aspect of the original design – loss of head in the outflow section and significantly increased the efficiency and degree of reactivity (compared of previous layouts equipped with the draft tube where the effect of suction was absent due to the ventilation process and an improper shape of the runner case). Further development of the cross-flow turbine was determined in two main directions .The direction was reconstruction of the suction section (especially by redesigning the runner casing and adding the draft tube), and the second direction was connected with optimisation of nozzle and guide vane shapes.

This contribution presents results of flow pattern computations through two cross-flow turbines.

The first machine is an example of classical solution (impulse turbine without a suction section), the second one is a new design (reaction turbine with a draft tube). The comparison is based on a two-dimensional analysis performed by means of the code FLUENT 5.0™.

2. Principle of operation

A classical cross-flow turbine consists of two main parts, a nozzle and a runner.

The main characteristic feature of a cross-flow turbine is the water jet of rectangular cross-section, which passes twice through the blade cascade. Water flows through the runner blades first from the periphery towards the centre, and then, after crossing the internal space, from the inside outwards. This machine is therefore a double stage turbine and the water fills only a part of the runner at a time [2]. In the cross-flow turbines with the low degree of reactivity, which are with acceptable accuracy called impulse turbines, the pressure in the water jet doesn't change substantially during the flow through the runner ducts [1]. Therefore, the water stream discharged from the runner is under the same pressure as at the inlet. As it was mentioned before, in Cink's constructions and derivative ones, a higher degree of reactivity is obtained by means of applying the draft tube and resigning of the ventilation. As a consequence of these modernisation, the difference in the pressure between the inlet and outlet parts of the runner occurs, and the water jet is accelerated in this area. In the reactive mode of operation, the suction effect of the draft tube has a significant influence on the utilisation of the energy.

A graphical view of the flow through a cross-flow turbine is shown in Figure 2.

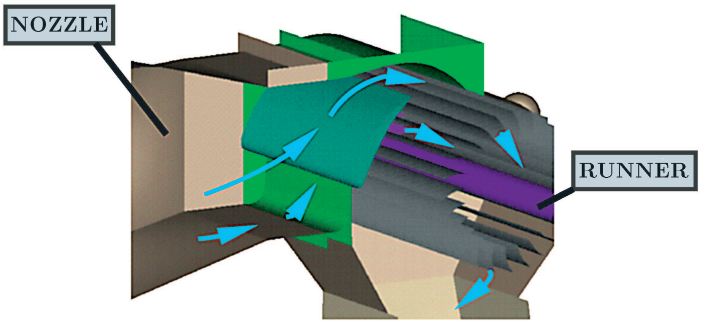

Figure 2. Schematic of the flow pattern through a cross-flow turbine

3. Technical data of the analysed turbines

Both model cross-flow turbines under investigation were designed at the Institute of Fluid Flow Machinery of the Polish Academy of Sciences. Geometrical and operating parameters of both cross-flow turbines are presented in Tables 1 and 2.

Table 1. Impulse turbine (the first design) SSH-300/150

Geometrical parameters of the turbine	Parameters of the rated operating point
– outer diameter of the runner $d_1 = 300$mm – inner diameter of the runner $d_2 = 200$mm – width of the runner $l = 150$mm – number of blades $z = 30$ – blade thickness $\delta = 3.6$mm – inlet and outlet angles $\beta_1 = 150^\circ$ and $\beta_2 = 90^\circ$	– head $H = 15$m – flow rate $Q = 0.195\text{m}^3/\text{s}$ – output $N = 23$kW – nominal speed $n = 550$rpm – guide vane opening $a_0 = 85\%$

Table 2. Reaction turbine TPP-300/300

Geometrical parameters of the turbine	Parameters of working point
– outer diameter of the runner $d_1 = 300$mm – inner diameters of the runner $d_2 = 200$mm – width of the runner $l = 300$mm – number of blades $z = 30$ – blade thickness $\delta = 3.6$mm – inlet and outlet angles $\beta_1 = 150^\circ$ and $\beta_2 = 90^\circ$	– head $H = 10$m – flow rate $Q = 0.3\text{m}^3/\text{s}$ – nominal speed $n = 410$rpm – guide vane opening $a_0 = 85\%$

4. Numerical computation of the flow

General purposes of numerical computation of the flow through the SSH-300/150 and TPP-300/300 turbines included determination of the fields of pressure and velocity, and finally specification of their efficiency in different points of operation. The analysis was conducted on two dimensional models in the whole area of flow – from the inlet stub pipe to the outflow part of both turbines. Computations in the third (axial) dimension were omitted because of the invariability of the flow channel geometry in this direction. This step decreased somehow the accuracy of the results, but on the other hand reduced substantially the time of calculations. The analysis was performed using the FLUENT 5.0™ solver [3], which is based on the finite volume method.

4.1. Grid generation

In the process of grid generation two software tools were used. The AUTOCAD™ design program was applied to build the initial geometry of the flow systems of both the turbines. Grids were generated by the GAMBIT™ program. In the whole area of flow, the author applied the unstructured triangular grid. This decision resulted from substantial deformations of the structural grid in many crucial areas of the flow field. In the areas of higher gradients of analysed parameters, higher density of the grid was used to obtain the acceptable level of solution. A graphical view of the computational grid is shown in Figure 3.

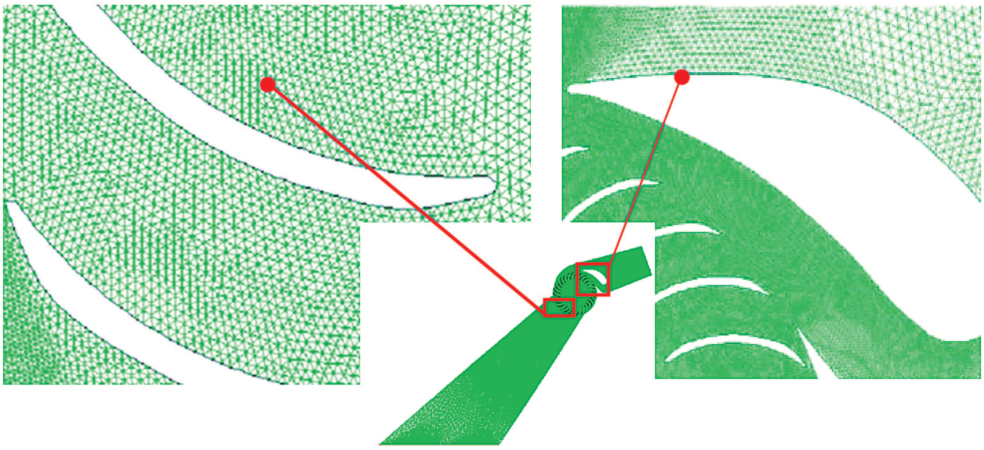

Figure 3. Computational grid with enlarged areas of higher concentrations of elements

4.2. Boundary conditions

In both cases of computations, uniform pressure inlet boundary conditions were used to define the fluid pressure at the flow inlet. In the incompressible flow, the inlet total pressure and the static pressure, are related to the inlet velocity by Bernoulli's equation. Hence, the velocity magnitude and the mass flow rate could be assigned at the inlet boundary.

Also outlet conditions for both cases were similar. The absolute static pressures were defined at the outflow of the turbines. Precise data for boundary conditions are presented in Table 3.

Table 3. Boundary conditions

Impulse turbine SSH-300/150	Reaction turbine TPP-300/300
Inlet conditions	
P_t – absolute total pressure $P_t = \rho g H + P_g = 248\,342\,\mathrm{Pa}$ P_g – gauge pressure (in this case atmospheric pressure), $101\,325\,\mathrm{Pa}$ ρ – density of water, $999.1\,\mathrm{kg/m^3}$ g – acceleration of gravity, $9.81\,\mathrm{m/s^2}$ H – head, 15m	P_t – absolute total pressure $P_t = \rho g H + P_g = 199\,336\,\mathrm{Pa}$ P_g – gauge pressure (in this case atmospheric pressure), $101\,325\,\mathrm{Pa}$ ρ – density of water, $999.1\,\mathrm{kg/m^3}$ g – acceleration of gravity, $9.81\,\mathrm{m/s^2}$ H – head, 10m
Outlet conditions	
P_c – absolute static pressure $P_c = P_g = 101\,325\,\mathrm{Pa}$	P_c – absolute static pressure $P_c = P_g + \rho g H_1 = 103\,285\,\mathrm{Pa}$ H_1 – difference of levels between the draft tube outlet and the tail water, 0.2m

4.3. Flow field in the rotating elements of the turbine

To analyse the flow in the rotating elements of the turbine, the FLUENT 5.0™ Moving Reference Frame option was used. The calculations were performed in the domain moving with the runner. In this case, the flow was referred to the rotating frame of reference, which simplified the analysis. As the consequence of such simplifications, unsteady problems such as wicket gate/runner interactions couldn't be modelled. As no averaging process of the inflow parameters at the interface between the rotating and stationary zone was applied, computations were performed in the entire flow field. The noticeable trace of rotation was an additional term of acceleration in the momentum equations. The left hand side of the momentum equations written in terms of relative velocity took the form:

$$\frac{\partial}{\partial t}(\rho \boldsymbol{v}_r)+\nabla(\rho \boldsymbol{v}_r \boldsymbol{v}_r)+2\boldsymbol{\Omega}\times\boldsymbol{v}_r+\boldsymbol{\Omega}\times\boldsymbol{\Omega}\times\boldsymbol{r}=\rho\boldsymbol{F}+\nabla T, \tag{1}$$

where $\boldsymbol{\Omega}$ – rotation vector, $\boldsymbol{v}_r$ – relative velocity and $\boldsymbol{r}$ – radius.

4.4. Turbulence model

In the computation process the Renormalization Group (RNG) k-ε Turbulence Model was used. Unlike the standard k-ε model, the RNG-based k-ε turbulence model is derived from the instantaneous Navier-Stokes equations. The idea of this model is to eliminate the direct influence of small-scale eddies through some mathematical procedures. This treatment reduces computational requirements for solving the system of Navier-Stokes equations. In the presented examples the turbulence intensity and hydraulic diameters were used to describe the parameters of the model.

4.5. Definition of the efficiency

The hydraulic efficiency of the cross-flow turbines was determined using the basic water turbine equation:

$$P_t=\omega\cdot T=\rho\cdot\omega\cdot\left(\int_A c_r\cdot c_u\cdot r\cdot dA\right), \tag{2}$$

where P_t – turbine power at the shaft, ω – angular velocity, T – torque at the shaft, ρ – density of water, c_r – radial component of the absolute velocity at the runner periphery, c_u – peripheral component of the absolute velocity at the runner periphery, A – peripheral surface of the runner and r – outer radius of the runner.

The hydraulic efficiency is the ratio between the power at the shaft and the power lost by water passing through the turbine:

$$\eta=\frac{T\cdot\omega}{g\cdot H\cdot\rho\cdot Q}, \tag{3}$$

where g – acceleration of gravity, H – head and Q – discharge.

Equation (3) can be rewritten in the discrete form for the 2D flow through a cross-flow turbine as:

$$\eta=\frac{\omega\cdot r\cdot b\cdot\left(\sum_{i=1}^{k_1} c_{ri}\cdot c_{ui}\cdot\Delta A_i\right)}{g\cdot H\cdot Q}, \tag{4}$$

where k_1 – number of the elements at the runner periphery, b – width of the runner and ΔA_i – length of a single element.

5. Results of computation

The performed analysis of the flow through the SSH-300/150 model turbine shows that the runner operates in pumping regime on a part of its perimeter. This effect can block the flow and influence the outflow conditions (turbulization of the jet in the part of the runner chamber). A visualisation, which was carried out at a laboratory test rig [4] (Institute of Fluid Flow Machinery of the Polish Academy of Sciences in Gdansk) confirms the results of numerical computations. In the area B (Figure 4) the intensive vortex structure appears, as a result of back flow in the runner chamber.

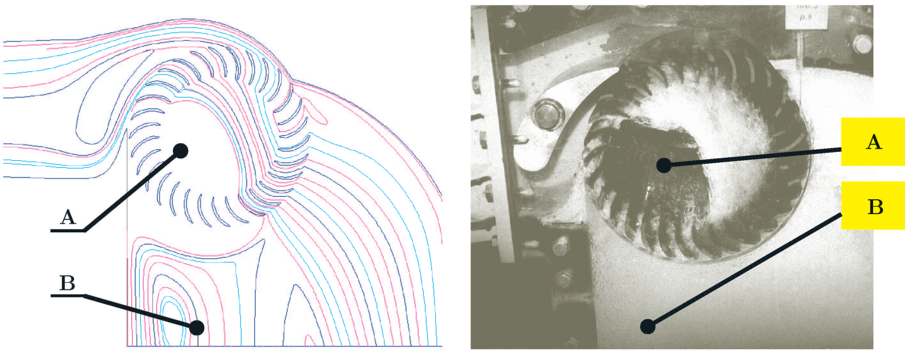

Figure 4. Distributions of the streamlines in the SSH-300/150 model turbine and a photograph from the experiment

Additionally, the computation results show the dead flow field in the internal part of the runner. This phenomenon is characteristic for this type of water turbines [5] and is easily discernible in the photograph (area A). In order to increase the significance of the numerical results, the author conducted computations of the efficiency curve (Figure 5) for the geometrical and operating parameters, presented in Table 1 and Table 2.

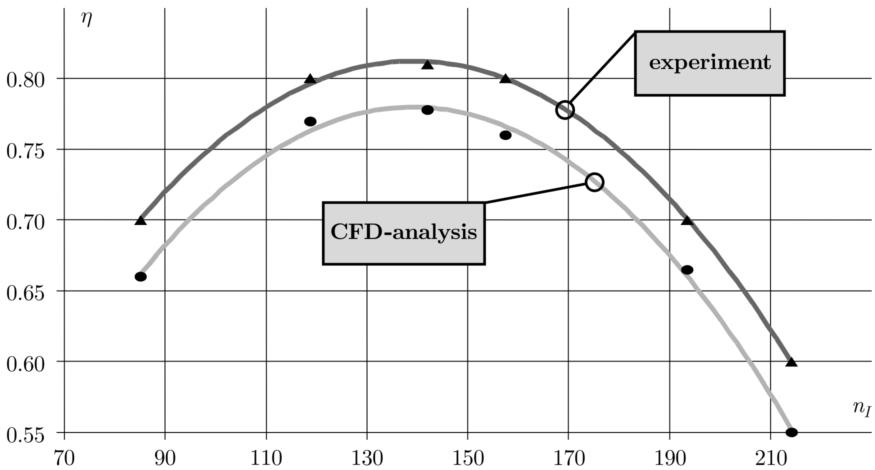

Figure 5. Efficiency curve of the SSH-300/150 model turbine

Some differences in the efficiency measured [4] and calculated can be caused by ventilation that was not taken into account in the CFD analysis.

The newly designed cross-flow turbine is equipped with a suction part (draft tube) and a runner casing redesigned in order to reduce the influence of pumping effects in the runner. The computations carried out for this turbine show the proper distributions of streamlines in the draft tube for the optimum point of operation. No separation or other flow disturbance can be noticed inside the draft tube. The efficiency of the newly designed turbine is comparable with that of the old one although it should be borne in mind that differently defined net heads are used. The efficiency of the turbine TPP-300/300 is presented as a function of rotation speed n_I under the head of $H = 15\,\mathrm{m}$, which is derived from the equation:

$$n_I = \sqrt{\frac{H}{H'}} \cdot n\,, \tag{5}$$

where head of operating for TPP-300/300 turbine $H' = 10\,\mathrm{m}$ and n – speed.

The efficiency curves and distributions of streamlines and velocities are shown in Figures 6, 7 and 8.

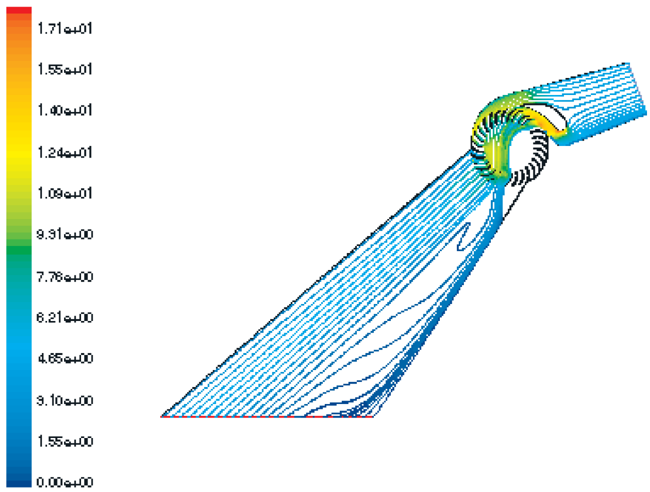

Figure 6. Distribution of streamlines in the TPP-300/300 model turbine

6. Conclusion

The use of CFD analysis to aid the design of cross-flow hydraulic turbines has been shown. The main purpose of the numerical computations of the SSH-300/150 impulse cross-flow turbine was validation of the numerical procedure by means of comparison with the results of a laboratory experiment. The newly designed TPP-300/300 cross-flow turbine has been equipped with a draft tube, which fulfils an important function of utilising the difference in specific energy between the runner bottom edge and the tail water surface. The loss of head due to this difference, especially in the case of low head machines, may reach the proportions, which cannot be tolerated. The numerical computations performed on a new design show that the

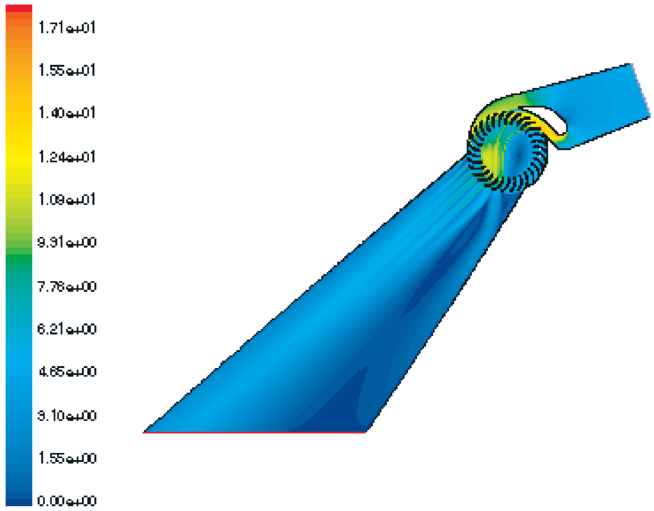

Figure 7. Distribution of velocities in the TPP-300/300 model turbine

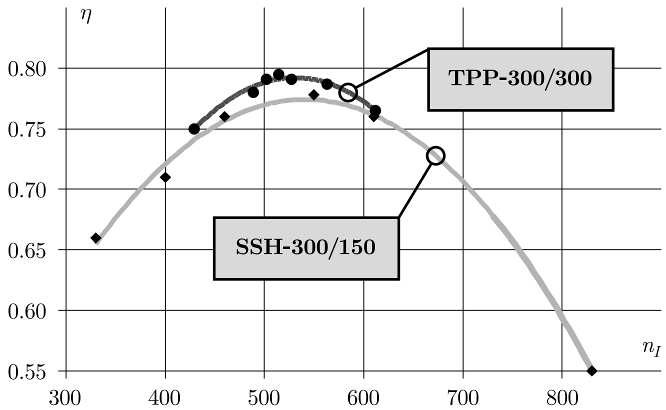

Figure 8. Comparison of computed efficiency curves of the TPP-300/300 and SSH-300/150 model turbines

properly designed draft tube reduces some undesirable phenomena like backflows and separations.

Acknowledgements

The analysis was performed under the Research Project no. 7 T07C 032 17 of the Committee of Scientific Research directed by prof. M. Zarzycki from Technical University of Silesia. The title of the project is "Analysis of the selected operating properties of the cross-flow turbines".

References

[1] Varga J 1959 *Acta Technica Academiae Scientiarum Hungaricae* **XXVII** 79
[2] Fukutomi J and Nakase Y 1985 *Bulletin of JSME* **28** (241) 1436
[3] 1998 *Fluent 5.0, User's guide*, Fluent Inc., USA
[4] Reymann Z 1993 *Reports of the IMP PAN*, Gdansk, Poland, No.467/1363/93, pp. 23–24 (in Polish)
[5] Reymann Z, Steller K and Litorowicz J 1989 *Trans. IF-FM* **90–91** 87